

# Focused-Ion-Beam Fabrication of Slots in Silicon Waveguides and Ring Resonators

Jonathan Schrauwen, *Student Member, IEEE*, Jeroen Van Lysebetsens, Tom Claes, *Student Member, IEEE*, Katrien De Vos, *Student Member, IEEE*, Peter Bienstman, *Member, IEEE*, Dries Van Thourhout, *Member, IEEE*, and Roel Baets, *Fellow, IEEE*

**Abstract**—We present the focused-ion-beam fabrication of slots in existing silicon waveguides and racetrack resonators. The etch process was conducted with iodine enhancement and an alumina hard mask. We demonstrate a propagation loss of 100 dB/cm for slot waveguides and a Q value of 850 for slot racetrack resonators with bend radius of 6  $\mu\text{m}$ .

**Index Terms**—Focused ion beam, resonator, silicon, slot waveguide.

## I. INTRODUCTION

SLOT waveguide structures have recently attracted much attention because of their ability to tightly confine light in a material with low refractive index [1], [2]. As opposed to resonant confinement schemes, introducing a slot in a high index waveguide, such as a silicon waveguide, enables broadband confinement in a low index material. Slot structures amplify the interaction between tightly confined optical modes and low index contrast materials, which is of great interest for various devices such as sensors, modulators, etc. The silicon-on-insulator platform is attractive for the fabrication of these devices. A variety of silicon photonic components have been successfully fabricated with deep ultraviolet (UV) optical lithography (248 or 193 nm) and dry etching [3], [4], which is compatible with standard processes used for the fabrication of the most advanced electronic circuits and allows for high volume manufacturing. However, the typical size of a slot in a silicon waveguide is of the order of 100 nm, which is a challenge for current optical lithography techniques [5]. Therefore, most of the demonstrated prototype slot structures were fabricated by electron beam lithography and dry etching [2], [6].

An alternative prototyping technology is the focused ion beam (FIB) technique. This technique offers superior flexibility because of its direct write capability. There is no need for a resist no dry etching step, and one can easily alter existing devices (which is difficult with resist-based methods). On the

contrary, similar to electron beam writing, FIB is a serial technique and therefore inherently not adequate for high volume fabrication of devices. However, one can envisage a medium volume production scheme if FIB is used for small modifications to structures that are fabricated with optical lithography, which is the pursued approach in this letter. This fabrication scheme enables the fabrication of angled trenches and slits and structures with more complex 3-D geometries [7]. Furthermore, because the ion beam can be focused in a spot of about 10 nm, features smaller than 50 nm can be fabricated.

FIB etching of silicon is not straightforward because of the optical losses brought about by crystal damage and implanted impurities. Several approaches were proposed to alleviate this hurdle. Furnace annealing at temperatures above 800 °C reduces the losses due to evaporation and out-diffusion of impurities and due to crystal regeneration [8]. However, such high temperatures are not compatible with metals, polymers, and III–V semiconductors that are potentially present in finished devices. Therefore, this approach cannot be used for device modifications. An alternative approach is FIB etching in the presence of an etch rate-enhancing chemical compound such as iodine [9], [10]. By the presence of a thin layer of nonvolatile etch products (mainly silicon–iodide species) the silicon is partly protected from the impinging ions, whereas the etch rate is increased by at least a factor of ten. After removal of the nonvolatile etch products by baking at 300 °C this process yields structures with relatively low optical losses. Due to the limited maximum temperature of the process it can be applied on most finished devices. A similar process, using a hot sample stage, was recently developed for FIB etching of InP with iodine enhancement [11].

In this letter, we first discuss the optimization of the slot width by simulation, then we present the FIB fabrication of slots by iodine enhanced FIB etching in deep-UV prefabricated waveguides and racetrack resonators, and finally we demonstrate a measured propagation loss of 100 dB/cm for a straight slot waveguide and a Q value of 850 for a slot ring resonator with slot widths of respectively 90 and 120 nm.

## II. SIMULATION

In this letter, we use a silicon-on-insulator substrate with 220-nm silicon membrane on top of a 2- $\mu\text{m}$  oxide buffer layer. Simulations are performed in CAMFR, a freely available eigenmode expansion tool [12]. All simulations were performed with water as top cladding, targeting sensing applications.

First, we have determined the substrate leakage losses as a function of slot width and total waveguide width. The results

Manuscript received July 02, 2008; revised September 04, 2008. First published October 31, 2008; current version published November 21, 2008. This work was supported in part by the European Union through the Network of Excellence ePIXnet and the Fund for Scientific Research (FWO). The work of T. Claes and K. De Vos was supported by the the Institute for the Promotion of Innovation by Science and Technology in Flanders (IWT) under a grant.

The authors are with the Department of Information Technology (INTEC), Ghent University—IMEC, B-9000 Gent, Belgium (e-mail: Jonathan.Schrauwen@intec.ugent.be).

Color versions of one or more of the figures in this letter are available online at <http://ieeexplore.ieee.org>.

Digital Object Identifier 10.1109/LPT.2008.2006001

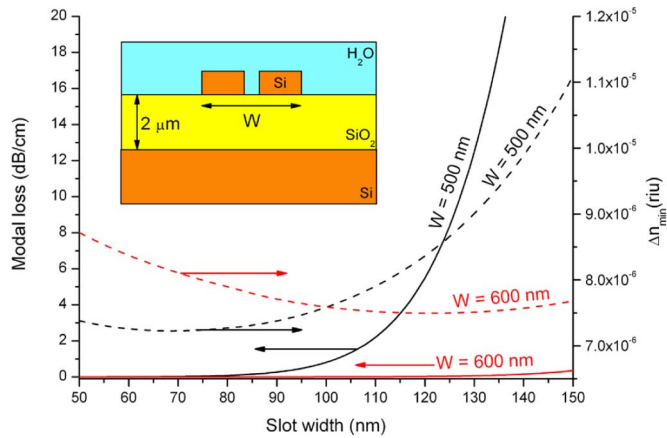


Fig. 1. (Left axis) Simulated modal loss due to substrate leakage through the 2- $\mu\text{m}$  bottom oxide cladding, as a function of slot width for 500- and 600-nm wide wires. (Right axis) Minimally detectable change in refractive index of the top water cladding.

are presented in Fig. 1 (left vertical axis). For 500-nm waveguides the losses increase dramatically for slot widths in excess of 100 nm because the mode size increases; in 600-nm waveguides the losses are more than one order of magnitude lower. Nevertheless, these substrate leakage losses are far lower than the measured material absorption losses (see the following). Another important optimization parameter is the mode overlap with the top cladding material, i.e., the aqueous region shown in the inset of Fig. 1, which determines the sensitivity of resonance wavelength shifts on changes of refractive index in this material. The results of this simulation are presented on the right vertical axis in Fig. 1, supposing that the minimally detectable resonance wavelength shift is 5 pm, at a wavelength of 1550 nm. For 600-nm wires the optimum slot width is around 120 nm, for 500 nm it is about 70 nm.

### III. FABRICATION WITH FIB

The slots were fabricated in an FEI Nova Nanolab 600, with a gallium focused ion beam current of 50 pA and acceleration voltage of 30 keV, corresponding to a beam size of about 30 nm. In previous work, we have demonstrated relatively low loss devices with 90-nm slits and vertical sidewalls by using alumina as hard etch mask and iodine as selective etchant [7]. Similarly, an alumina layer of 50 nm was first deposited on the deep-UV fabricated waveguides. Due to the limited penetration depth of gallium ions this thickness is sufficient to protect the sample during ion imaging and alignment procedures. Furthermore, the etch rate selectivity is sufficient (more than ten) to guarantee nearly vertical sidewalls of the etched slots. The slits were etched through alumina and silicon in one step using iodine etch enhancement. The width of the slit can be varied by adjusting the etch dose or by using a higher beam current and thus larger beam size. Since the bottom oxide is also etched by this process—albeit slower than silicon—the slot depth is also affected by this variation. Nearly vertical sidewalls of FIB etched structures can also be obtained by using suspended silicon membranes [13], but this complicates the fabrication procedure and limits flexibility. After FIB etching the sample was baked on a

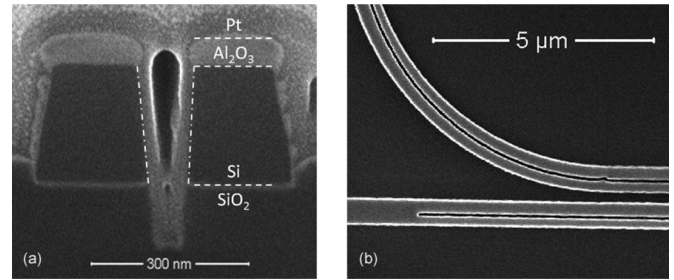


Fig. 2. (a) Cross-sectional micrograph (after Pt deposition) of an FIB etched 90-nm wide slot in a 500-nm wide waveguide. The dashed-dotted lines highlight the slot edges. (b) Top view micrograph of part of an FIB etched slot in an access waveguide and racetrack resonator. The inadequate alignment can be improved by using more complex alignment strategies.

hotplate in  $N_2$  for 2 h at 300 °C to remove the nonvolatile silicon-iodide layer [10].

Alignment of the etched slot on the existing waveguides and rings was performed by making ion microscopy images and visually overlaying the slots. The precision of this technique was limited because of the 12-bit digital scan generator in our machine (the size of the grid is the field of view divided by 4096). A higher magnification increases the alignment accuracy; but to be able to etch a slot in a racetrack resonator (with bend radius of 6  $\mu\text{m}$  and straight sections of 3  $\mu\text{m}$ ) without stitching, a field of view of 25.6  $\mu\text{m}$  was chosen. The patterns were defined with a digital scan algorithm, with a dwell time of 400 ns and a pitch of 3 nm. To etch straight slots with a length of 30, 40, and 50  $\mu\text{m}$  a single stitch was used. Fig. 2(a) shows a cross-sectional micrograph of a 90-nm slot in a 500-nm wide waveguide (Pt was deposited *in situ* before cross sectioning). This slot was etched in the presence of adsorbed iodine on the surface, in 170 000 passes, where each point is etched for 400 ns per pass. This corresponds to an etch dose of 1.1  $\mu\text{C}/\text{cm}$ . The 90-nm one was the thinnest slot we could obtain with a beam current of 50 pA and beam size of 30 nm.

The same process was used to etch a slot in a 600-nm wide racetrack resonator. However, in this case, the number of passes was 275 000, which brings the total etch dose to 1.83  $\mu\text{C}/\text{cm}$  (total etch time was about 2 min). The measured slot width was 120 nm. Fig. 2(b) shows a top view micrograph of part of the etched slot in access waveguide and racetrack resonator. The evident alignment errors are mainly caused by the simple visual alignment procedure and can be alleviated by using more complex alignment strategies implementing image recognition and multipoint alignment of the write field. However, this was beyond the scope of this work.

### IV. MEASUREMENT AND DISCUSSION

The devices were characterized in a fiber-to-fiber transmission measurement. The setup consists of polarization controlled light from a tunable laser that is coupled in and out of tapered broad waveguides by near vertically positioned fibers and grating couplers. A droplet of water was placed on top of the fabricated devices to provide the aqueous top cladding.

The propagation losses of the straight slot waveguides were calculated by linear regression of the loss through device lengths from 10 to 50  $\mu\text{m}$ , as displayed in Fig. 3 (top). The plotted

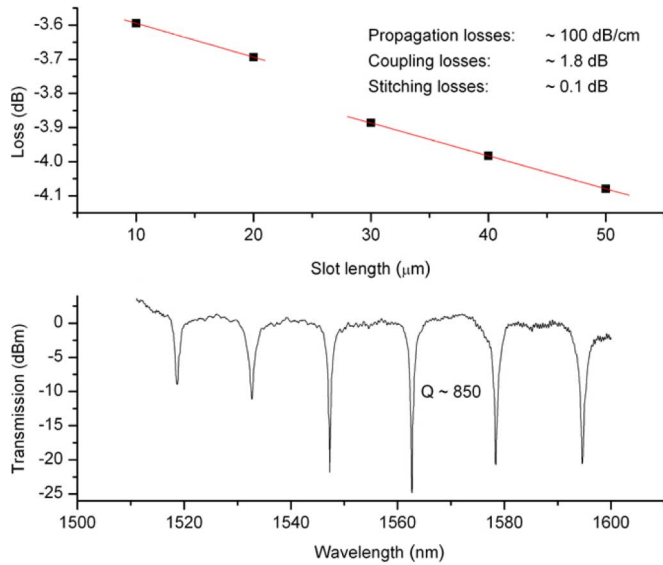


Fig. 3. Top: transmission measurements of 90-nm wide slots etched in a 500-nm wide silicon waveguide yield a propagation loss of 100 dB/cm. Bottom: transmission spectrum of a 600-nm wide racetrack resonator with 120-nm wide slot. We have measured a Q value of about 850 and an extinction ratio of 25 dB.

data points are the average values of two consecutive measurements of four identical samples. A distinction between slots up to 20  $\mu\text{m}$  and longer ones can be made: shorter slots were written in one field of view, longer ones were stitched once. The result is a propagation loss of 100 dB/cm, a coupling loss between waveguide and slot waveguide of 1.8 dB, and a stitch loss of 0.1 dB. The propagation loss of 100 dB/cm can—according to simulations—be attributed to a 10-nm-thick damaged layer with an absorption coefficient of  $1650\text{ cm}^{-1}$ , similar to what was reported for implanted waveguides [10]. These losses are not as low as previously reported for electron beam fabricated slot waveguides (about 10 dB/cm [6]). However, since FIB is a serial technique, the length of etched devices for prototyping purposes is not likely to exceed 100  $\mu\text{m}$ . This yields a 1-dB loss per device, which is acceptable. Furthermore, FIB can be used to etch slots in existing waveguides, which is difficult with resist-based methods such as electron beam lithography.

The normalized transmission spectrum of the fabricated slot racetrack resonator is displayed in Fig. 3 (bottom). The dips in the spectrum clearly indicate resonance in the racetrack with bend radius of 6  $\mu\text{m}$ . A Q value of about 850 and an extinction ratio of 25 dB were measured around 1560 nm, suggesting that the device is operating near critical coupling. From simulations it can be expected that round trip losses for this ring are dominated by propagation losses, with smaller contributions from bend losses and mode mismatch between straight and bent sections. However, calculation of the round trip losses from the various resonance dips in this measurement has led to inconclusive results. Although the Q value is likely to increase after high temperature annealing, the current process is attractive as rapid prototyping technique, e.g., for the design verification of high-sensitivity biosensors. Furthermore, the iodine terminated silicon surface present in the slot can be of interest for localized functionalization [14].

## V. CONCLUSION

We report the direct focused-ion-beam etching of slots in pre-fabricated waveguides and racetrack resonators, with the use of iodine etch enhancement. The experimentally measured propagation loss is 100 dB/cm for a 90 nm wide slot; the calculated Q-factor for a resonator with bend radius of only 6  $\mu\text{m}$  is about 850. The developed process is of interest for rapid prototyping and design verification of silicon slot devices.

## ACKNOWLEDGMENT

The authors would like to thank L. Van Landschoot for fabrication support.

## REFERENCES

- [1] Q. Xu, V. R. Almeida, R. R. Panepucci, and M. Lipson, "Experimental demonstration of guiding and confining light in nanometer-size low-refractive-index material," *Opt. Lett.*, vol. 29, no. 14, pp. 1626–1628, 2004.
- [2] V. R. Almeida, Q. Xu, C. A. Barrios, and M. Lipson, "Guiding and confining light in void nanostructure," *Opt. Lett.*, vol. 29, no. 11, pp. 1209–1211, 2004.
- [3] W. Bogaerts, R. Baets, P. Dumon, V. Wiaux, S. Beckx, D. Taillaert, B. Luyssaert, J. V. Campenhout, P. Bienstman, and D. V. Thourhout, "Nanophotonic waveguides in silicon-on-insulator fabricated with CMOS technology," *J. Lightw. Technol.*, vol. 23, no. 1, pp. 401–412, Jan. 2005.
- [4] S. Selvaraja, P. Jaenen, S. Beckx, W. Bogaerts, P. Dumon, D. V. Thourhout, and R. Baets, "Silicon nanophotonic wire structures fabricated by 193 nm optical lithography," in *Proc. LEOS Annu. Meeting, U.S.*, 2007.
- [5] E. Jordana, J.-M. Fedeli, P. Lyan, J. P. Colonna, P. Gautier, N. Daldosso, L. Pavesi, Y. Lebour, P. Pellegrino, B. Garrido, J. Blasco, F. Cuesta-Soto, and P. Sanchis, "Deep-UV lithography fabrication of slot waveguides and sandwiched waveguides for nonlinear applications," in *Proc. IEEE Group IV Photonics 2007*, pp. 1–3.
- [6] T. Baehr-Jones, M. Hochberg, C. Walker, and A. Scherer, "High-Q optical resonators in silicon-on-insulator-based slot waveguides," *Appl. Phys. Lett.*, vol. 86, p. 081101, 2005.
- [7] J. Schrauwen, F. V. Laere, D. V. Thourhout, and R. Baets, "Focused-ion-beam fabrication of slanted grating couplers in silicon-on-insulator waveguides," *IEEE Photon. Technol. Lett.*, vol. 19, no. 11, pp. 816–818, Jun. 1, 2007.
- [8] Y. Tanaka, M. Tymczenko, T. Asano, and S. Noda, "Fabrication of two-dimensional photonic crystal slab point-defect cavity employing local three-dimensional structures," *Jpn. J. Appl. Phys.*, vol. 45, pp. 6096–6102, 2006.
- [9] J. Schrauwen, D. V. Thourhout, and R. Baets, "Focused-ion-beam fabricated vertical fiber couplers in silicon-on-insulator waveguides," *Appl. Phys. Lett.*, vol. 89, p. 141102, 2006.
- [10] J. Schrauwen, D. V. Thourhout, and R. Baets, "Iodine enhanced focused-ion-beam etching of silicon for photonic applications," *J. Appl. Phys.*, vol. 102, p. 103104, 2007.
- [11] V. Callegari, P. M. Nellen, J. Kaufmann, P. Strasser, F. Robin, and U. Sennhauser, "Focused ion beam iodine-enhanced etching of high aspect ratio holes in InP photonic crystals," *J. Vac. Sci. Technol. B*, vol. 25, no. 6, pp. 2175–2179, 2007.
- [12] P. Bienstman and R. Baets, "Optical modelling of photonic crystals and VCSELs using eigenmode expansion and perfectly matched layers," *Opt. Quant. Electron.*, vol. 33, pp. 327–341, 2001.
- [13] W. C. L. Hopman, F. Ay, W. Hu, V. J. Gadgil, L. Kuipers, M. Pollnau, and R. M. de Ridder, "Focused ion beam scan routine, dwell time and dose optimizations for submicrometre period planar photonic crystal components and stamps in silicon," *Nanotechnology*, vol. 18, p. 195305, 2007.
- [14] W. Cai, Z. Lin, T. Strother, L. M. Smith, and R. J. Hamers, "Chemical modification and patterning of iodine-terminated silicon surfaces using visible light," *J. Phys. Chem. B*, vol. 106, pp. 2656–2664, 2002.